



**HAL**  
open science

# A methodology for weld bead geometry and operating conditions determination in Wire Arc Additive Manufacturing

Diego Verbist, Matthieu Museau, Frederic Vignat, Sylvain Lavernhe

## ► To cite this version:

Diego Verbist, Matthieu Museau, Frederic Vignat, Sylvain Lavernhe. A methodology for weld bead geometry and operating conditions determination in Wire Arc Additive Manufacturing. 12th JCM 2024 - 33rd INGEGRAP International - Research and Innovation in Graphic Engineering: Tools for Achieving Sustainable Development Goals and Addressing Emerging Global Challenges, Jun 2024, Valencia (Espagne), France. hal-04618527

**HAL Id: hal-04618527**

**<https://hal.science/hal-04618527>**

Submitted on 20 Jun 2024

**HAL** is a multi-disciplinary open access archive for the deposit and dissemination of scientific research documents, whether they are published or not. The documents may come from teaching and research institutions in France or abroad, or from public or private research centers.

L'archive ouverte pluridisciplinaire **HAL**, est destinée au dépôt et à la diffusion de documents scientifiques de niveau recherche, publiés ou non, émanant des établissements d'enseignement et de recherche français ou étrangers, des laboratoires publics ou privés.

# A methodology for weld bead geometry and operating conditions determination in Wire Arc Additive Manufacturing

Diego Verbist<sup>1</sup>, Matthieu Museau<sup>1</sup>, Frederic Vignat<sup>1</sup>, Sylvain Lavernhe<sup>2</sup>

<sup>1</sup> Univ. Grenoble Alpes, CNRS, Grenoble INP, G-SCOP

<sup>2</sup> Université Paris-Saclay, ENS Paris-Saclay, LURPA, 91190, Gif-sur-Yvette, France  
diego.verbist@grenoble-inp.fr

**Abstract.** When manufacturing a part using Directed Energy Deposition (DED) processes such as Wire Arc Additive Manufacturing (WAAM), it is necessary to determine the deposition path and operating parameters (wire feed speed, torch speed, energy). While the operating parameters influence the geometry of the manufactured beads, the deposition trajectory impacts the way in which these beads are arranged to fill the target shape. The strong dependence of the bead geometry on the thermal conditions (which are difficult to accurately manage) makes the choice of adequate parameters complicated. The problem can be tackled in various ways, and this paper proposes a method for determining the trajectory and operating parameters from the current state of the part (simulated or measured) and manufacturing or geometric constraints. The proposed methodology is divided into 2 phases:

- 1- Determination of acceptable bead geometries based on geometric constraints and the current state of the part.
- 2 - Determination of the operating conditions required to obtain an acceptable bead, based on a phenomenological model of bead shape.

**Keywords:** WAAM, geometry control, Near Net Shape, parameter configuration, thermal simulation, phenomenological model.

## 1 Introduction

Wire-Arc-Additive-Manufacturing (WAAM), classified under the ISO/ASTM 52900:2021 standard, is a technique that involves the use of an electric arc as the energy source to melt a metallic wire used as the feedstock. The molten metal is deposited on a base substrate and solidifies to form a weld bead. By piling up layers of these weld beads, the process can create both thin walls and voluminous structures.

This technology allows for a greater material deposition rate relative to other Additive Manufacturing (AM) processes, allowing for the production larger scale parts, quicker and with greater energy efficiency. Additionally, certain welding regimes such as Cold Metal Transfer (CMT) allow for a lower heat input which reduces heat accumulation problems during the process. CMT's stable deposition was also proven to help reduce porosity problems in the case of aluminium alloys [1].

One of the main challenges with WAAM is the production of parts in a Near-Net-Shape scope. This concept consists in producing the parts as close as possible to their

final geometry [2], with the goal of reducing material waste and diminishing the need for finishing operations.

The part geometry depends on the geometry of the individual weld beads that are used to build it. The size and shape of these weld beads can be influenced by the amount of material that is deposited, which is directly dependent on the ratio between Wire Feed Speed (WFS) and Torch Speed (TS).

Proper control of the weld bead geometry heavily relies on accurately managing the thermal environment during deposition. Limousin et al. [3] established heat accumulation and uneven heat distribution during the process as a main cause of geometrical defects.

Thermal management during the process is problematic due to the large number of phenomena influencing the thermal environment, mainly the characteristics of the material, the thermal state and geometry of the substrate as well as the behaviour of the heat source. This renders the choice of process parameters for the goal geometry a complex task.

In this article we aim to propose a methodology to manufacture Near-Net-Shape parts on CMT-based WAAM. The methodology, shown in Fig.1 consists of two steps:

1. Assessing the situation of the current layer; mainly, the goal part geometry, the current substrate geometry, and user-defined allowance limits in order to establish weld bead geometry constraints. These constraints are then used to definite mathematical criteria of acceptability for the possible weld bead geometries. These criteria are in turn used to determine a space of acceptable weld bead geometries for the current layer.
2. Establishing the link between weld bead geometry and physical process parameters. Using this link to transform the space of acceptable geometries of into a corresponding space of acceptable process parameters.

By following this methodology, we hope to provide a systematic approach aiming to produce Near-Net-Shape parts using WAAM, thereby reducing material waste and the amount of finishing operations required to obtain the final geometry.

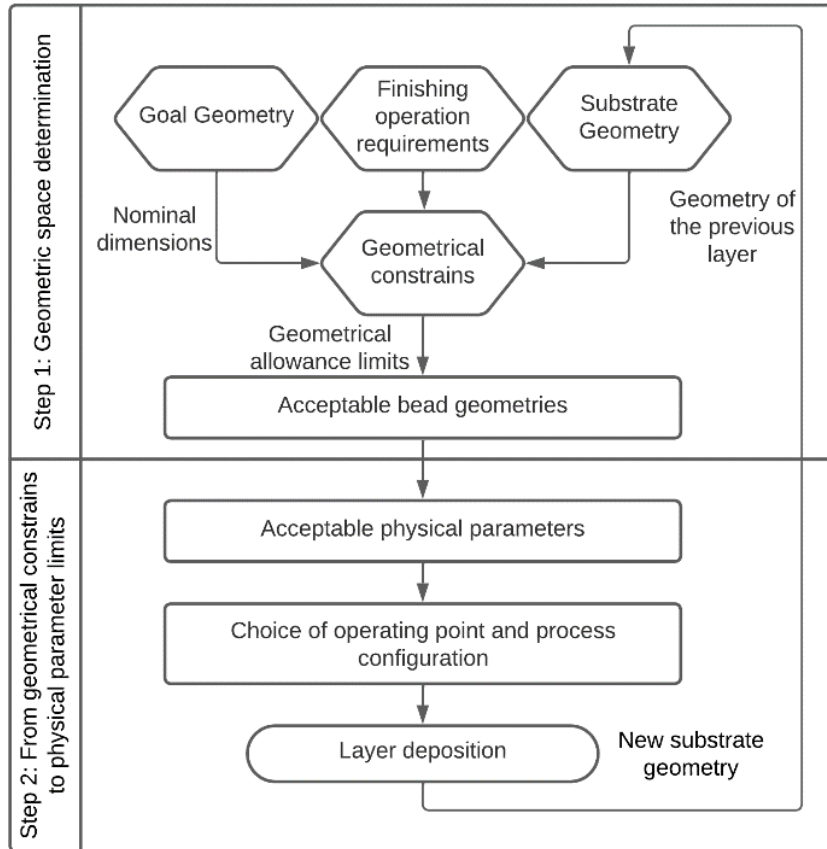
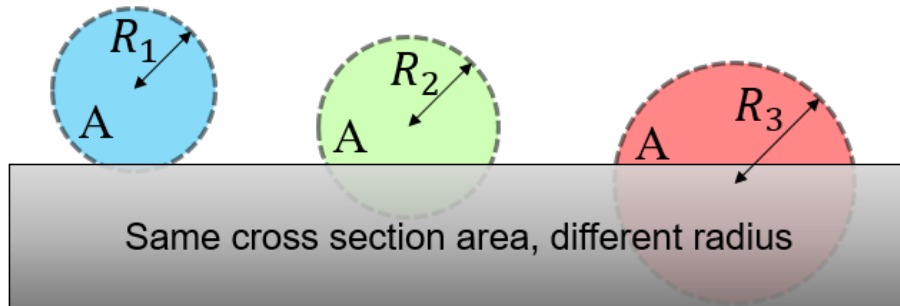


Fig. 1. Diagram of the proposed methodology

## 2 Determination of the geometrical space

### 2.1 Modelling the weld beads

To study and manage weld bead geometries, it is necessary to use a model to approach the shape of weld beads. A number of different weld bead geometry approximation models were proposed in the literature. Xiong et al. [4] as well as Ding et al. [5] studied the parabola, circular arc and sine function models, determining them as reliable approximations of the weld bead profile. In our work, following the footsteps of Limousin et al. [3] the weld beads were analysed using the circular arc model. This allows us to define the geometry of any given weld bead by using only 2 parameters: the radius  $R$  and the cross-section area  $A$ . An example of different weld bead geometries can be seen in Fig.2.



**Fig. 2.** Circular arc weld bead model.

When piling up these weld beads, the cross-section area that is evaluated is the area of the circle minus the area of the superposition with previously deposited beads. As seen on Fig.3, where the cross-section area of the top bead is coloured in green.

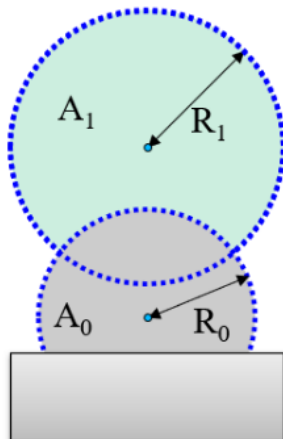


**Fig. 3.** Vertical overlap of two beads with circular section

## 2.2 Part geometry and geometrical constraint goals

After defining the weld bead model that will be used to fill the desired shape, it is time to define the goal part shape and the geometrical constraints that will condition the choice of weld bead geometries. In most cases the parts can be classified as either thin-wall structures (which can be created by vertically piling up single weld beads) and voluminous parts (which require more than one bead to be piled up side by side). This means that two possible case scenarios can be defined for the weld beads that we aim to deposit. These can be seen in Fig.4.

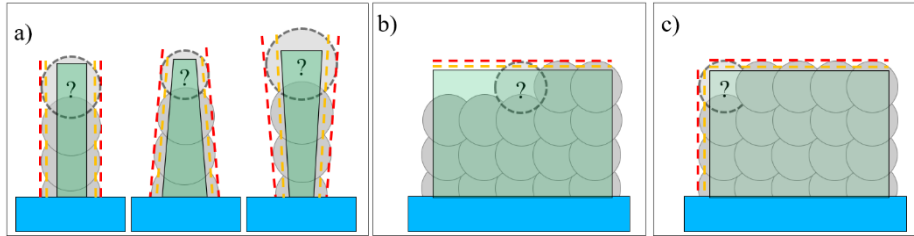


**Fig. 4.** Bead piling case scenarios to fill the design space coloured in green. a) Vertical stacking of single beads. b) multi-bead horizontal cladding far from borders. c) multi-bead horizontal cladding near the part's borders.

These two cases are subjected to different geometrical constraints. In the case single-bead vertical stacking (Fig.4.a), the predominant constraints are related to machining allowance limits. In Fig.4 design space (i.e., the final goal geometry for the part) is coloured in green, while the orange lines represent a minimal machining allowance limit that is added to ensure proper conditions for finishing operations. The area enclosed by the orange lines should therefore be completely filled with material. Finally, maximal allowance limits can be defined to represent Near-Net Shape constraints, meaning the weld beads shouldn't cross the boundaries represented by the red lines.

For multi-bead cladding (Fig.4.b), each weld bead is also subjected to geometrical constraints. The main geometrical constraints guiding the choice of weld bead geometries would be a flatness constraint. This constraint implies that the weld beads should be chosen and placed in a way that ensures that the top surface of the given layer will remain mostly flat, offering adequate conditions for the deposition of the next layer. To maintain this flatness constraint, studies in the literature proposed finding an optimal centre distance between beads that would improve process stability, and therefore the top layer's flatness. Notably, Ding et al. [6] developed a Tangent Overlapping model (TOM), which allows prediction of a "critical centre distance" with neighbouring beads, which was shown to successfully improve geometrical stability of the deposited walls. Finally, when the bead is near the borders of the design space, the machining allowance limits can still be applied.

These geometrical constraints can be represented by mathematical expressions which can be calculated based only on the design space dimensions and the chosen allowance values as well as the geometry of the substrate. This will be illustrated with the following case study.

### 2.3 Case study: a wall with increasing thickness

In the context of this article, the methodology was applied to the case study of a wall with increasing thickness (Fig.5), which will be used to illustrate the different steps.

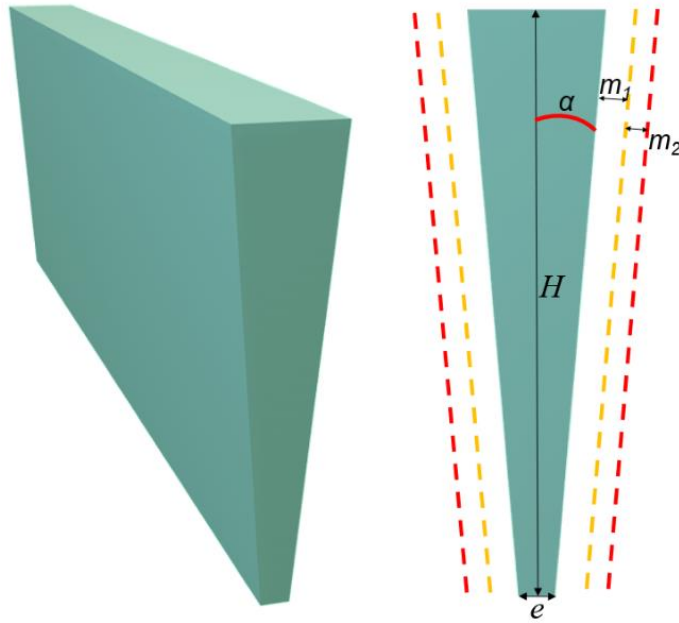


**Fig. 5.** Goal geometry for the use case: design space in green, minimal machining allowance in orange and maximal allowance in red.

This type of geometry can be defined by 3 variables: the initial width  $e$ , the total height  $H$  and the slope angle  $\alpha$ . Then the geometrical constraints are represented by the coloured lines that are parallel to the border of the design space. The distance between these lines and the design space is given by the chosen values  $m_1$  and  $m_2$ . Usually,  $m_1$  will be set at a value of at least 0.8mm to ensure proper conditions for surface finishing. Meanwhile  $m_2$  can be chosen by the user depending on their aim to reduce the need for finishing operations and material waste.

Once the geometrical limits are established, we can start defining criteria of acceptability for the weld beads. First, we determine the limits of weld bead radii for each layer:

- The weld beads must completely cover the area encased by the minimal allowance limits. Given the slope of the wall, since the thickness increases from one layer to the next, we decided to establish the previous bead's radius as the minimal radius for the new bead (Fig.6.a).
- Since the beads have to respect the maximum allowance limit, the bead with the biggest possible radius will be tangent to the maximum allowance limits and it will also coincide with the intersection of the previous bead with the minimum allowance limit. (Fig.6.b)
- Any weld bead radius between these limits is considered acceptable (Fig.6.c)

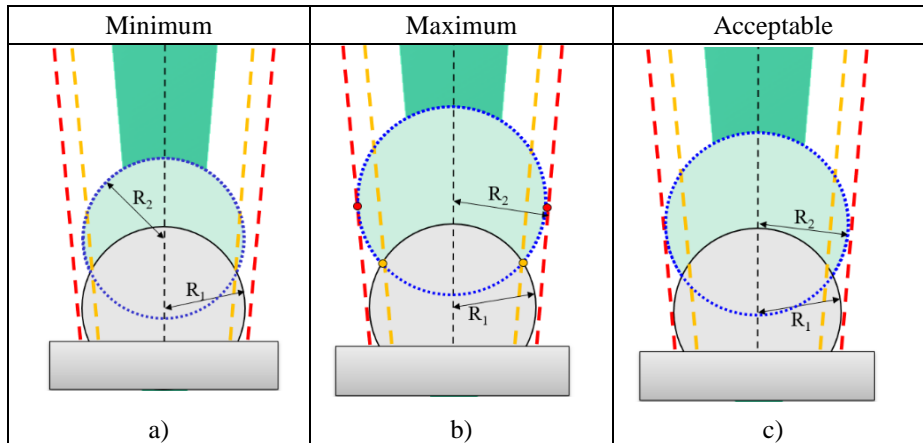


**Fig. 6.** Limits of bead radii corresponding to the geometrical constraints.

Then, for each value of radius between the limits, different centre positions can be acceptable, as long as the allowance constraints are respected. We can then define:

- A lowest acceptable position, when the bead surpasses the maximum allowance limit (Fig.7.a)
- A highest acceptable position, intersection of the new and old weld beads coincides with the minimal allowance limit line (yellow line), going higher would leave the area encased by the yellow line uncovered. (Fig.7.c)
- Any weld bead centre position between these limits is acceptable. (Fig.7.b)

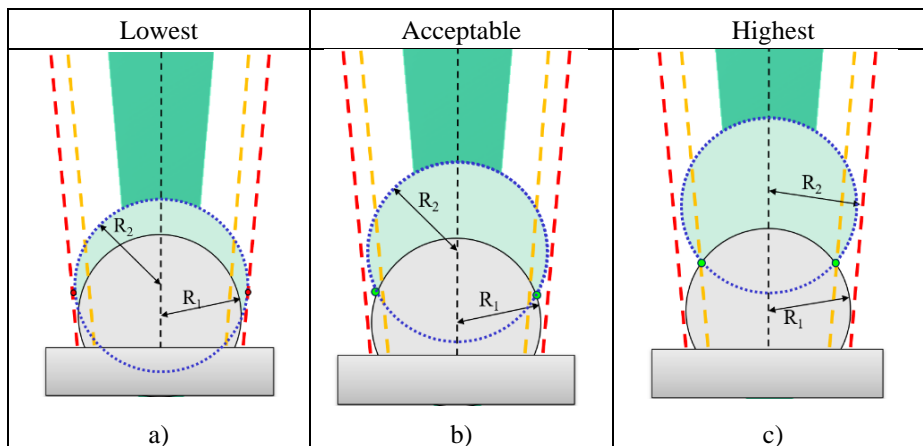


**Fig. 7.** Limits of bead cross section area for a given radius.

Each centre position, for any given radius, will change the weld bead cross section area, therefore these geometrical constraints restrict the weld bead radii and cross section areas of our weld beads.

All of these limits can be calculated as a function of the centre height and radius of the previous bead (i.e., the current state of the substrate), the goal geometry dimensions and the allowance constraints. Notably, the limits depend on the substrate geometry: either the base plate or the geometry that is inherited from the previous layer.

Given that these limits can be expressed as a function of the design space dimensions, the substrate geometry and the allowance limits. It is possible to mathematically obtain a so called “*acceptable zone*” of weld bead geometries that fit the constraints for any given layer (Fig.8). Every point within the boundaries of this zone represents a weld bead geometry that respects the previously established constraints.

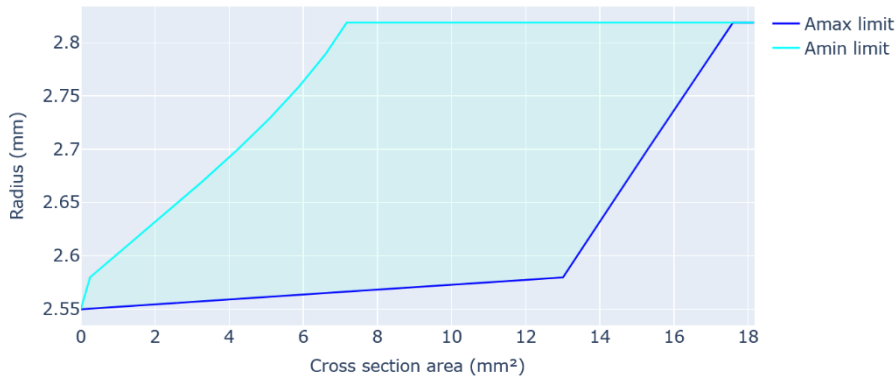


**Fig. 8.** Acceptable zone of weld bead geometries for the second layer of the case study. Given the initial parameters  $e = 5$ ,  $\alpha = 5^\circ$ ,  $m_1 = 0.8$  mm,  $m_2 = 0.5$  mm and the geometry of the previous weld bead described by the  $R_0 = 2.55$  mm and a centre elevation  $Z_0 = 0$  mm.

Additionally, the cross-section area of a weld bead can be considered to be directly proportional to the ratio WFS/TS. Dividing the cross-section area of the weld bead by the cross-section area of the wire feedstock (constant) results in the value of the ratio WFS/TS. Therefore, any limits in weld bead cross-section area can easily be converted into limits in WFS/TS.

### 3 Process parameters for the acceptable beads

#### 3.1 The influence of thermal conditions

Once this acceptable zone of weld bead geometries has been found, the aim of the study shifts towards finding the process parameters that would produce acceptable beads. For this it is necessary to evaluate the influence of different process parameters on the geometry of the deposited weld beads. Previous work by Limousin et al. [3] as well as Chergui et al. [7] established that one of the main factors influencing the geometry of the weld beads is the thermal environment during the deposition.

In this previous work, a representative parameter of the thermal environment during the deposition was defined. This parameter (named  $T_{dep}$  after Deposition Temperature) is obtained by finite element thermal simulation of the weld bead during deposition

(Fig.9) and corresponds to the average temperature of a section of the temperature field located at the front of the weld bead (highlighted area in Fig.9.b).

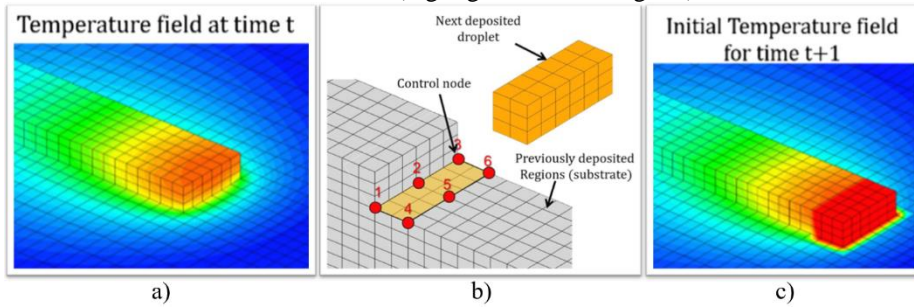


**Fig. 9.** Main steps of the element deposition technique [7 & 3].

In order to study the relationship between process parameters and the resulting weld bead geometry, a series of experiments was realised, with similar protocols to the ones presented by Limousin et al. [2]. A number of aluminium weld beads with different WFS/TS ratios were deposited in different thermal conditions. The weld bead geometries (Radii) were obtained by 3D scanning and thermal simulations were used to obtain the corresponding stable  $T_{dep}$ .

Using these results, a phenomenological model was created to represent the relationship between the weld bead geometries (Radius) and process parameters (WFS/TS and  $T_{dep}$ ). This model can be seen on Fig.10.a in the shape of a 3D response surface representation.

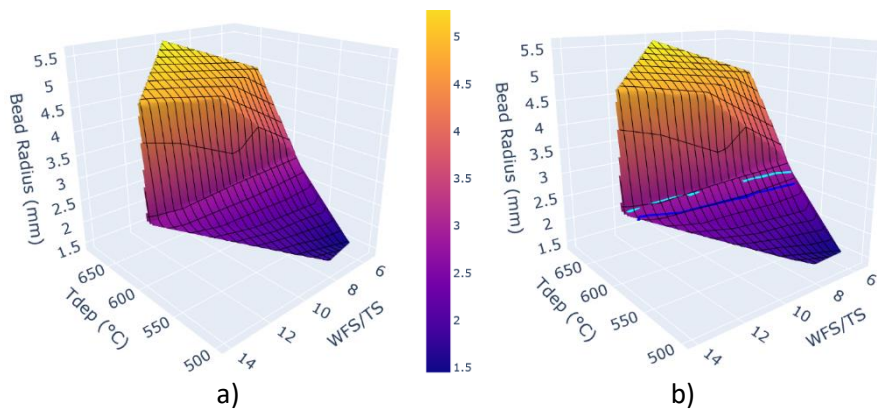


**Fig. 10.** Phenomenological model: Radius,  $T_{dep}$  and WFS/TS.

This model can be used as the first step to transform the geometrical limits from Fig.9 into process parameter limits. For this, as seen on Fig.10.b, the acceptable zone of radius and cross-section area was projected onto the model's surface (cross-section area converted into WFS/TS). The delineated green area represents the range of

acceptable operating conditions. Fig.11 depicts the projection of this area on the  $T_{dep}$  and WFS/TS axes.

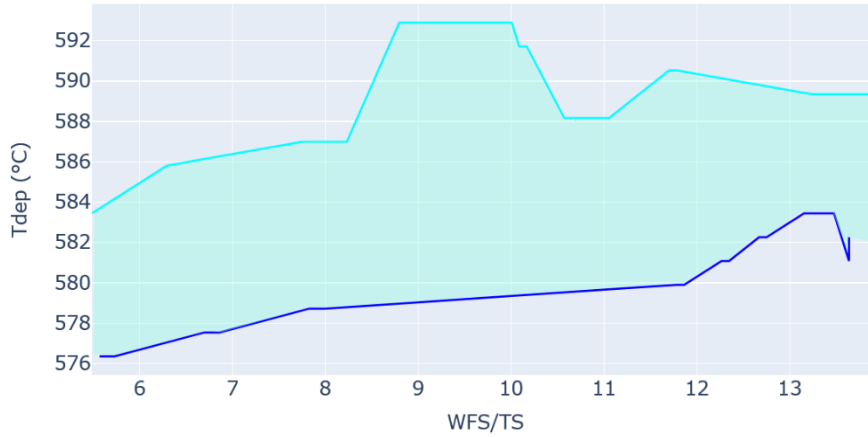


**Fig. 11.** Acceptable area of  $T_{dep}$  and WFS/TS parameters.

Additionally, based on electrical measurements during the experiments, it was also possible to associate the operating points of weld bead cross-section and deposition temperature to a value of electrical power output (which were calculated as the product of the measured voltage and current values). Based on this, a new 3D surface linking the deposition temperature to the bead cross-section area and the arc power was created, as shown in Fig.12.a.

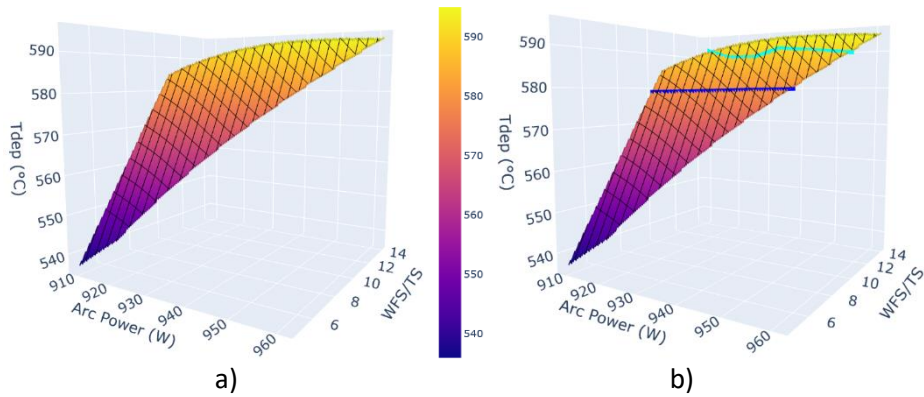


**Fig. 12.** Response surface ( $T_{dep}$ , WFS/TS, Power)

Fig.12.b shows the projection of the acceptable zone ( $T_{dep}$  and WFS/TS) from Fig.11 onto the new response surface. The resulting delineated area of the surface contains the operating points of  $T_{dep}$ , Power and WFS/TS corresponding to the acceptable geometries which were determined in Section 1. This delimited zone is shown plotted in Fig.13 on the WFS/TS and Arc Power axes (the representation on Fig.13 was cut so as to only show the part of the graph where both curves are present).

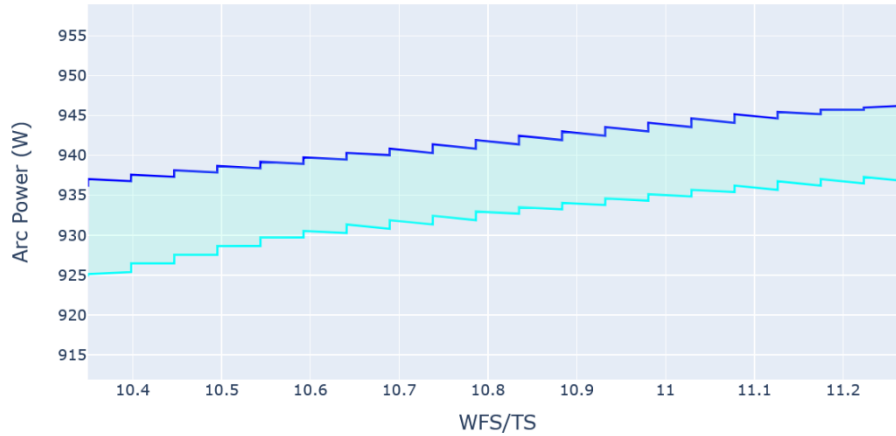


**Fig. 13.** Acceptable zone in the Power and WFS/TS axes.

This area delimited by these blue lines contains the pairs of Arc Power and WFS/TS parameter values that would verify the geometrical constraints that we set for the given layer of the wall.

The operating point can then be chosen inside the acceptable area following different criteria depending on the aims of the user. For higher certainty of compliance, the choice should be as far as possible from the boundaries of the acceptable zone.

After deposition of the given layer, 3D scanning of the new substrate geometry will produce a digital model which will be used in the following iteration of the methodology to calculate new geometrical constraints for the next weld bead.

Repeating this process for each layer should allow to systematically obtain the desired layer geometries.

## Conclusion

As seen throughout the case study, the proposed methodology enables the transformation of geometrical constraints into limits of physical process parameters for WAAM. The iterative method should enable building, layer by layer, a part that fits the goal geometrical constraints.

In the case of CMT-based WAAM processes, the power of the heat-source is not directly controllable by the user. This is due to the built-in synergy system which controls the operation of the welding station. This system ensures a stable welding process and adapts both the arc power and the wire feed speed automatically to follow the short-circuit cycles of Cold Metal transfer welding. This however, renders the prediction and control of the real arc power and wire feed speed values difficult. Because of this, future perspectives of our work include establishing the link between these physical parameters (power and wire feed speed) and the process parameters that can be directly configured by the user, such as Contact Tube to Work-piece Distance (CTWD) [8] and the

individual values of WFS and TS (while maintaining the desired ratio for ideal deposition rate).

Additionally, studies will be run in order to adapt this methodology to new part geometries, such as multi-bead walls (Fig4.b & Fig.4.c) as well as shapes requiring a more dynamic variation of bead width inside a given layer.

## References

1. Cong, B., Ding, J., Williams, S. Effect of arc mode in cold metal transfer process on porosity of additively manufactured Al-6.3%Cu alloy. *International Journal of Advanced Manufacturing Technology*, 76(9–12), 1593–1606 (2015).
2. Cominotti, R., Gentili, E. Near net shape technology: An innovative opportunity for the automotive industry. *Robotics and Computer-Integrated Manufacturing*, 24(6), 722–727 (2008).
3. Limousin, M., Manokruang, S., Vignat, F., Museau, M., Grandvallet, C., Béraud, N. Effect of temperature and substrate geometry on single aluminium weld bead geometry deposited by Wire Arc Additive Manufacturing: Proposition of an experimental procedure. *CIRP Journal of Manufacturing Science and Technology*, 45, 61–68. (2023).
4. Xiong, J., Zhang, G., Gao, H., & Wu, L. Modeling of bead section profile and overlapping beads with experimental validation for robotic GMAW-based rapid manufacturing. *Robotics and Computer-Integrated Manufacturing*, 29(2), 417–423. (2013).
5. Ding, D., He, F., Yuan, L., Pan, Z., Wang, L., & Ros, M. The first step towards intelligent wire arc additive manufacturing: An automatic bead modelling system using machine learning through industrial information integration. *Journal of Industrial Information Integration*, 23. (2021).
6. Ding, D., Pan, Z., Cuiuri, D., & Li, H. A multi-bead overlapping model for robotic wire and arc additive manufacturing (WAAM). *Robotics and Computer-Integrated Manufacturing*, 31, 101–110. (2015).
7. Chergui, A., Villeneuve, F., Béraud, N., & Vignat, F. Thermal simulation of wire arc additive manufacturing: a new material deposition and heat input modelling. *International Journal on Interactive Design and Manufacturing*, 16(1), 227–237. (2022).
8. Hölscher, L.V., Hassel, T. & Maier, H.J. Detection of the contact tube to working distance in wire and arc additive manufacturing. *International Journal of Advanced Manufacturing Technology* **120**, 989–999 (2022)